



Sterile neutrinos: some or all of dark matter?

THESIS

submitted in partial fulfillment of the
requirements for the degree of

BACHELOR OF SCIENCE

in

PHYSICS

Author :	Ole Moors
Student ID :	2047055
Supervisor :	Dr. A. Boyarsky
2 nd corrector :	Dr. V. Cheianov

Leiden, The Netherlands, July 10, 2020

Sterile neutrinos: some or all of dark matter?

Ole Moors

Huygens-Kamerlingh Onnes Laboratory, Leiden University
P.O. Box 9500, 2300 RA Leiden, The Netherlands

July 10, 2020

Abstract

After a short introduction on the history of dark matter research, we review the current state of knowledge on both dark matter and sterile neutrinos, motivating sterile neutrinos as a dark matter candidate. We then investigate the dependence of current constraints on the sterile neutrino parameter space on the fraction χ_N of the dark matter mass density that is due to sterile neutrinos, and derive a lower bound on the fraction assuming the 3.5 keV spectral line detected in galaxies and galaxy clusters is caused by sterile neutrino decay: $\chi_N \gtrsim 0.1$.

Contents

1	Introduction	7
2	Dark matter and its properties	11
2.1	Properties of dark matter	11
2.2	Tremaine-Gunn bound	12
3	Active and sterile neutrinos	15
3.1	The active neutrinos	15
3.2	Sterile neutrinos	18
3.2.1	The seesaw mechanism	18
3.2.2	Sterile neutrinos as dark matter	21
3.2.3	Sterile neutrinos as Warm Dark Matter	24
4	Sterile neutrinos as a fraction of dark matter	27
4.1	Tremaine-Gunn bound	27
4.2	X-ray constraints	28
4.3	Thermal overproduction	29
5	Discussion and conclusion	33

Chapter 1

Introduction

In 1933, Swiss astronomer Fritz Zwicky did a strange discovery [1, 2]. He measured the so-called velocity dispersion $\sigma^2 = \langle v_x^2 \rangle \approx \langle v_y^2 \rangle \approx \langle v_z^2 \rangle$ of the galaxies in the Coma galaxy cluster. He then also used the virial theorem for gravitationally bound systems,

$$\langle T \rangle = -\frac{1}{2} \langle V \rangle, \quad (1.1)$$

where T is the total kinetic energy and V is the total potential energy of the system, to estimate the velocity dispersion of the cluster with its measured total mass, using $T \approx \frac{3}{2} M \sigma^2$ and a rough approximation for V . To his surprise, the velocity dispersion calculated this way was significantly lower than the one observed. Zwicky hypothesised that this discrepancy could be caused by some kind of invisible massive matter: he called it "dunkele materie", or dark matter.

Since then, more evidence has been found for the existence of Zwicky's dark matter. The mass of elliptical galaxies has also been calculated using their velocity dispersion (stars in elliptical galaxies move in random orbits), and the masses found were up to 10 times bigger than one would expect from the galaxies' visible matter alone [3]. In spiral galaxies, stars tend to orbit in the same direction in the same plane, and a relationship can be derived for the orbital velocity of the stars at a radius R from the center:

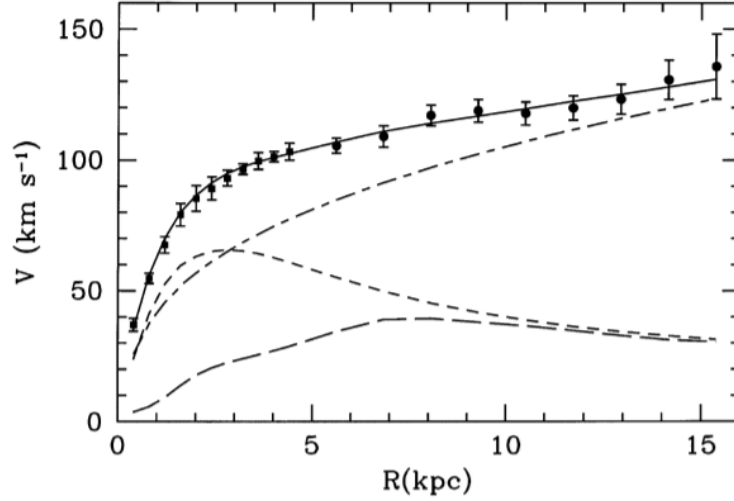


Figure 1.1: Rotation curve of the galaxy M33. The short-dashed line is the rotation curve calculated from stellar mass only, the long-dashed line is the curve from gaseous mass only, and the dot-dashed line is the curve from the missing mass only. Figure taken from Ref. [4].

$$v_{circ}(R) = \sqrt{\frac{GM(R)}{R}}, \quad (1.2)$$

where $M(R)$ is the total mass within a radius R and G is Newton's gravitational constant. Calculating $v_{circ}(R)$ this way by using the visible mass distribution of spiral galaxies and comparing it to the measured orbital velocities gives graphs like figure 1.1 [4]. As we can see, the actual rotation curve is not what we would expect at all from the visible mass alone: there seems to be a large ring of invisible mass around the center of the galaxy.

In 2002, the distribution of hot ($\sim 10^7$ K), X-ray emitting gas in the cluster Abell 2029 was investigated [5]. It was found that the measured amount of gas couldn't possibly be contained by the cluster's visible mass alone: another case of missing mass was found. Moreover, since it turned out that the vast majority of the mass of the cluster was dark matter, the distribution of dark matter in the cluster could be found from the gas distribution. The found distribution matched existing models for dark matter with generally non-relativistic momenta (cold dark matter) instead of generally relativistic momenta (hot dark matter).

Gravitational lensing has also been a useful tool in investigating dark mat-

ter. Strong gravitational lensing on galaxies has reaffirmed previous results [6], but weak gravitational lensing has paved the way for one of the most important studies in dark matter's history. In 2006, a rather unique event was studied: a merger of two galaxy clusters called the Bullet Cluster [7]. Using weak gravitational lensing, the mass distribution of the merger was measured, and not only was a mass discrepancy found, the center of mass of the merger was also significantly displaced from what was expected from the visible mass alone. Up until this point, theories predicting that the mass discrepancies were caused by a change in Newton's laws or the laws of gravity at galactic scales were also considered*, but none of them could explain the shift in the center of mass: the Bullet Cluster gave us the first true evidence that dark matter indeed exists, and that it is not just an illusion cast by unknown physical laws.

But the question remains: just what is this dark matter? Does it consist of undetectable asteroids, primordial black holes [11, 12], some sort of elementary particle, or a combination of the above [13]? It seems we can rule out anything made of baryons, including asteroids. In the early days of the universe, photons and baryons were bound together in the photon-baryon plasma. Acoustic waves travelled through this plasma, caused by the baryons in the plasma falling into gravitational potential wells and bouncing back out due to pressure caused by the resulting temperature increase. When the universe cooled off sufficiently, the baryons formed hydrogen nuclei, the photons flew away, and the plasma was no more. We can still see the photons today as the cosmic microwave background (CMB), and remnants of the acoustic waves are still visible as anisotropies in the temperature of the CMB.

The correlations between these anisotropies can be studied, and from them, we can derive the ratio between the mass of the baryons and the mass causing the gravitational potential wells. Using data of the CMB found by the Planck space telescope in 2013 [14], it has been found that just 15% of the mass in the universe is baryonic: the remaining 85% is the non-baryonic massive matter that caused the gravitational potential wells way back when. This ratio roughly corresponds to the visible matter-dark matter ratio we find in galaxies and galaxy clusters, which is a strong hint that the non-baryonic massive matter and (the majority of) dark matter might very well be one and the same. This also means dark matter must have played a role in structure formation in the early universe if it was present

*Mordehai Milgrom's Modified Newtonian dynamics (MOND) was an example of a theory describing a modification to Newton's laws [8–10].

way back then. The most widely accepted and successful model of how dark matter affected structure formation is the Λ CDM model, which has correctly predicted the evolution of the universe and its large-scale structure. It is sometimes called "the Standard Model of dark matter", and it is based on the assumption that dark matter is cold and has always been cold. However, another model, WDM (Warm Dark Matter), which is based on dark matter starting out hot and cooling down afterwards, has not yet been completely excluded [15].

This discussion does not rule out primordial black holes as a dark matter candidate, but for this thesis, sterile neutrinos were investigated as a possible candidate. Sterile neutrinos are the hypothetical right-handed chiral counterparts of "regular" (active) neutrinos, which to date have only been observed with left-handed chirality. Sterile neutrinos are called sterile because, contrary to active neutrinos, they do not couple to the weak interaction: the only interaction they couple to is gravity. This makes it incredibly hard to find evidence of the existence of the particle, and nearly impossible to measure it directly. Measurements have been done to find evidence of sterile neutrinos, but the results of the two biggest experiments show these efforts are far from conclusive: the IceCube Detector found no evidence of sterile neutrinos in 2016 [16], but the MiniBooNE experiment in 2018 did find evidence [17], although the significance of its results was 4.7σ , just below the necessary 5σ .

In this thesis, we motivate sterile neutrinos as a dark matter candidate and review the current state of sterile neutrino dark matter research: in chapter 2, we will discuss dark matter, and in chapter 3, we will discuss sterile neutrinos and their status as a dark matter candidate. Then, in chapter 4, we will discuss some of the various bounds on the properties of sterile neutrino dark matter, and answer the research question of this thesis: how do the Tremaine-Gunn bound, the X-ray constraints, and the thermal overproduction bound on the properties of sterile neutrino dark matter change if we assume not all dark matter consists of sterile neutrinos? We will do this by investigating how each of these bounds were obtained, and then rederiving them for the case where dark matter consists of other particles in addition to sterile neutrinos. Finally, we will conclude the thesis in chapter 5.

Dark matter and its properties

One might wonder why we would investigate hypothetical particles like sterile neutrinos as a dark matter candidate, when we have a large pool of already known particles in the Standard Model. However, no particle in the Standard Model could possibly be dark matter. In this chapter, we will discuss some of the properties a dark matter candidate must have*, and go over the arguments used to show that we need to look beyond the Standard Model to find the true nature of dark matter.

2.1 Properties of dark matter

There are several properties a dark matter candidate must have:

- It must be massive. Massless particles can exert gravity, according to general relativity, but they are inherently relativistic, which clashes with the results that point to dark matter being (somewhat) cold.
- It must be chargeless, or at most have an electric charge far smaller than the charge of the electron. A recent study [18] has shown that, if dark matter is entirely made of charged particles, their charge would satisfy $q/e \lesssim 10^{13\pm 1} mc^2/\text{GeV}$. So unless the mass of the particles is on the order of $\sim 1 \text{ ZeV}/c^2$ or larger (no known particle has a mass even close to this value), their charge must be very small indeed.
- It must have a production mechanism that can produce it in quantities that can explain the abundance of dark matter in the universe.

*Assuming most if not all of dark matter is made of this candidate.

- There must be some reason that dark matter is predominantly cold. The properties of any dark matter candidate, i.e. their production mechanism or the interactions they couple to, must be able to explain this.
- It must be stable on at least the timescale of the age of the universe

The Standard Model does not offer a very broad selection of massive, chargeless, very stable particles. In fact, only three known non-baryonic particles or composite particles fit these criteria: the three neutrinos. Neutrinos, however, have a very small mass. Therefore, a good first test to see if dark matter can consist of neutrinos is to find a lower bound on the mass of dark matter. Such a bound is called a Tremaine-Gunn bound.

2.2 Tremaine-Gunn bound

The original Tremaine-Gunn bound was derived by Scott Tremaine and James E. Gunn in 1979 [19]. They obtained their bound by assuming dark matter was fermionic and then comparing its phase-space distribution at different points in time using the Vlasov equation. However, we will use a different and somewhat simpler method to derive a bound. This bound will not be as strong as Tremaine and Gunn's, but it suits our purposes just fine, as we will see. The general formula for the bound has been previously derived by Alexey Boyarsky, Oleg Ruchayskiy and Dmytro Iakubovskiy [20], but we will repeat it here.

Neutrinos are fermions with spin $\frac{1}{2}$, so let's assume dark matter consists of such particles. Let's now (crudely) model a dark matter halo around a galaxy as free particles in a sphere with radius R , where R is the radius of the halo. The Pauli exclusion principle now implies (using the fact that dark matter is non-relativistic) that the highest energy a dark matter particle in this sphere has is the Fermi energy, $E_F = \frac{\hbar^2}{2m_{dark}} \left(\frac{3\pi^2 N}{V} \right)^{2/3}$, where N is the total number of particles in the halo, V is the volume of the halo, \hbar is the reduced Planck's constant, and m_{dark} is the mass of dark matter. Since dark matter is non-relativistic, this also implies that the highest velocity a dark matter particle has is the Fermi velocity:

$$v_F = \sqrt{\frac{2E_F}{m_{dark}}} = \frac{\hbar}{m_{dark}} \sqrt[3]{\frac{3\pi^2 N}{V}} \quad (2.1)$$

Now, for a stable halo, the Fermi velocity cannot exceed the escape velocity at the edge of the galaxy:

$$\frac{\hbar}{m_{\text{dark}}} \sqrt[3]{\frac{3\pi^2 N}{V}} < \sqrt{\frac{2GM}{R}}, \quad (2.2)$$

where M is the total mass of the galaxy. Now, using $V = \frac{4}{3}\pi R^3$ and $N = \frac{M}{m_{\text{dark}}}$ [†] and rewriting the inequality, we get:

$$m_{\text{dark}}^4 > \frac{9\pi\hbar^3}{8\sqrt{2}G^{3/2}M^{1/2}R^{3/2}} \quad (2.3)$$

This is the Tremaine-Gunn bound we will be using. It is strongly dependent on the galaxy we are considering, however. So let's consider the galaxy we know best: our own Milky Way. The total mass of the Milky Way has been estimated to be $(1.3 \pm 0.3) \times 10^{12} M_{\odot}$ [21], and its radius, including its dark matter halo, has been estimated in a very recent study to be 0.29 ± 0.06 Mpc [22]. Using these values, we find:

$$m_{\text{dark}} \gtrsim 4 \text{ eV}/c^2 \quad (2.4)$$

An upper bound on the combined mass of the three active neutrino flavors is [23]:

$$\sum_{\alpha=e,\mu,\tau} m_{\alpha} < 0.12 \text{ eV}/c^2, \quad (2.5)$$

a full order of magnitude lower than our Tremaine-Gunn bound. This excludes neutrinos from being dark matter, and confirms that we need to look beyond the Standard Model for dark matter candidates. Our research will focus on one particular candidate: sterile neutrinos.

[†]Not an unreasonable approximation, considering the abundance of dark matter in galaxies.

Active and sterile neutrinos

In this chapter, we will motivate the existence of sterile neutrinos, discuss some of their important properties and review what is already known about them as a dark matter candidate. But before we can do so, we must discuss some aspects of the active neutrinos first. For the rest of this thesis, we will work in natural units ($c = \hbar = 1$).

3.1 The active neutrinos

In the Standard Model, there are three charged leptons: the electron (e), the muon (μ), and the tau (τ). Each of these charged leptons has a corresponding active neutrino: the electron neutrino (ν_e), the muon neutrino (ν_μ), and the tau neutrino (ν_τ). They correspond to each other in the sense that each charged lepton can turn into its corresponding neutrino and vice versa by emitting or absorbing a W^- boson: this process is part of the basis of the weak interaction. Active neutrinos are chargeless, and they only couple to gravity and the weak interaction, which makes them notoriously difficult to detect. Also, unlike the other particles in the Standard Model, only neutrinos with left-handed chirality have been detected. The active neutrinos were also long thought to be massless, until neutrino oscillation was discovered.

Neutrino oscillation is the phenomenon where neutrinos seem to oscillate between the three flavors, instead of having one fixed flavor. The idea behind neutrino oscillation was developed primarily over the course of three articles published during the 1950s and 1960s that built on each other's

ideas: the first and third were written by Bruno Pontecorvo, and the second was written by Ziro Maki, Masami Nakagawa and Shoichi Sakata [24–26]. However, the phenomenon was not experimentally confirmed until much later: the Super-Kamiokande experiment provided the first clear evidence of neutrino oscillation in 1998 [27].

To explain why neutrino oscillation occurs, we will consider two neutrino flavors, ν_α and ν_β . We can think of these as eigenstates of the flavor operator, as they have a well-defined flavor. However, they don't necessarily also need to be eigenstates of the mass operator: the flavor operator and the mass operator might very well not commute. So suppose ν_1 and ν_2 are the mass eigenstates. If both sets of eigenstates are normalized, they are related to each other by a unitary transformation:

$$\begin{pmatrix} \nu_\alpha \\ \nu_\beta \end{pmatrix} = e^{i\psi} \begin{pmatrix} e^{i\varphi_1} \cos \theta & e^{i\varphi_2} \sin \theta \\ -e^{-i\varphi_2} \sin \theta & e^{-i\varphi_1} \cos \theta \end{pmatrix} \begin{pmatrix} \nu_1 \\ \nu_2 \end{pmatrix}$$

However, since ν_1 and ν_2 solve the Dirac equation,

$$(i\cancel{\partial} - m)\psi = 0, \quad (3.1)$$

because they are mass eigenstates, we can redefine them with an extra phase factor without affecting any physical results. The same holds for ν_α and ν_β due to their direct connection to the charged leptons (a result from quantum field theory: see e.g. [28]). It turns out that, by cleverly redefining each of the eigenstates with a different phase factor, we can eliminate all complex exponentials in the transformation matrix:

$$\begin{pmatrix} \nu_\alpha \\ \nu_\beta \end{pmatrix} = \begin{pmatrix} \cos \theta & \sin \theta \\ -\sin \theta & \cos \theta \end{pmatrix} \begin{pmatrix} \nu_1 \\ \nu_2 \end{pmatrix} \quad (3.2)$$

Now, consider a free ν_α neutrino produced at $t = 0$ travelling in the x -direction with momentum p . Then, at $t = x = 0$, the state of this neutrino is described by $|\psi(0)\rangle = |\nu_\alpha\rangle = \cos \theta |\nu_1\rangle + \sin \theta |\nu_2\rangle$, and at an arbitrary time and location:

$$|\psi(t, x)\rangle = \cos \theta |\nu_1\rangle e^{i(E_1 t - p x)} + \sin \theta |\nu_2\rangle e^{i(E_2 t - p x)}, \quad (3.3)$$

where the E_i are the energies of each mass eigenstate. In the limit $p \gg m_i$, where the m_i are the masses of the mass eigenstates (this limit typically

holds for neutrinos in the wild), we have $E_i = \sqrt{p^2 + m_i^2} \approx p + \frac{m_i^2}{2p}$. Now, at the neutrino's current location L , we have $t \approx x = L$, and:

$$|\psi(L)\rangle \approx \cos \theta |v_1\rangle e^{i\frac{m_1^2 L}{2p}} + \sin \theta |v_2\rangle e^{i\frac{m_2^2 L}{2p}}, \quad (3.4)$$

Now, if we try to measure the flavor of this neutrino, there is a chance that we measure v_β instead of v_α , equal to:

$$P_{\alpha \rightarrow \beta}(L) = |\langle v_\beta | \psi(L) \rangle|^2 \approx \sin^2(2\theta) \sin^2\left(\frac{\Delta m^2 L}{4p}\right), \quad (3.5)$$

where $\Delta m^2 \equiv m_2^2 - m_1^2$. So, as the neutrino moves, a small chance to be detected as a v_β neutrino instead of a v_α neutrino periodically appears and disappears if the mass difference between the two mass eigenstates is nonzero: this is neutrino oscillation.

For the three active neutrino flavors, the algebra becomes a bit more complicated, but the phenomena are very similar to the two-neutrino case. Let v_1 , v_2 and v_3 be the mass eigenstates. Then the general transformation between the two sets of eigenstates, while eliminating as many complex exponentials as possible, is:

$$\begin{pmatrix} v_e \\ v_\mu \\ v_\tau \end{pmatrix} = \begin{pmatrix} c_{12}c_{13} & s_{12}c_{13} & s_{13}e^{-i\delta} \\ -s_{12}c_{23} - c_{12}s_{23}s_{13}e^{i\delta} & c_{12}c_{23} - s_{12}s_{23}s_{13}e^{i\delta} & s_{23}c_{13} \\ s_{12}s_{23} - c_{12}c_{23}s_{13}e^{i\delta} & -c_{12}s_{23} - s_{12}c_{23}s_{13}e^{i\delta} & c_{23}c_{13} \end{pmatrix} \begin{pmatrix} v_1 \\ v_2 \\ v_3 \end{pmatrix} \quad (3.6)$$

Here, $c_{ij} \equiv \cos \theta_{ij}$ and $s_{ij} \equiv \sin \theta_{ij}$, where θ_{ij} is the mixing angle between v_i and v_j (in analogy to the angle θ in the two-neutrino case). This matrix is called the Pontecorvo-Maki-Nakagawa-Sakata (PMNS) matrix. Furthermore, the mass differences between all three mass eigenstates have been found to be nonzero, and they satisfy $\Delta m_{12}^2 \ll |\Delta m_{13}^2| \approx |\Delta m_{23}^2|$ [29]. From this, it follows that two different mass hierarchies are possible:

$$m_1 < m_2 < m_3 \quad (\text{Normal hierarchy})$$

$$m_3 < m_1 < m_2 \quad (\text{Inverted hierarchy})$$

In any case, this implies at least two active neutrinos must be massive.

However, as seen in equation (2.5), the combined mass of the three neutrinos has been measured to be less than 0.12 eV. This is considered quite unusual, since all other particles in the Standard Model are either massless or have masses around the MeV-GeV range. Nevertheless, a natural explanation for the low masses of can be found by introducing neutrinos with right-handed chirality, called sterile neutrinos.

3.2 Sterile neutrinos

Sterile neutrinos are chargeless spin- $\frac{1}{2}$ fermions, just like the active neutrinos. The major difference between the two is that sterile neutrinos don't couple to the W^\pm bosons, while the active neutrinos do: this is why they are called active and sterile. These properties arise because W^\pm only couple to fermions with left-handed chirality and antifermions with right-handed chirality. This means sterile neutrinos interact very weakly with the world around them: they only couple to gravity and the Z^0 boson. However, despite their ghostly nature, introducing them in a certain way can elegantly explain the low masses of their active brethren by means of an effect called the seesaw mechanism.

3.2.1 The seesaw mechanism

Imagine two massless spin- $\frac{1}{2}$ fermions with identical properties, except one has left-handed chirality (ψ_L), and one has right-handed chirality (ψ_R). They satisfy the Weyl equation:

$$\begin{cases} i\bar{\sigma}_\mu\partial^\mu\psi_L = 0 \\ i\sigma_\mu\partial^\mu\psi_R = 0 \end{cases} \quad (3.7)$$

Here, ψ_L and ψ_R are represented as two-component vectors called Weyl spinors, and we have $\sigma_\mu = (\mathbb{1}, \sigma_x, \sigma_y, \sigma_z)$ and $\bar{\sigma}_\mu = (\mathbb{1}, -\sigma_x, -\sigma_y, -\sigma_z)$, where the σ_i are the Pauli matrices. Now, if we want these fermions to be massive, there are two ways to add mass to the Weyl equation that keep the equation Lorentz covariant (which is required for a relativistic theory like this). The first is Dirac mass:

$$\begin{cases} i\bar{\sigma}_\mu\partial^\mu\psi_L = m\psi_R \\ i\sigma_\mu\partial^\mu\psi_R = m\psi_L \end{cases} \quad (3.8)$$

Or, if we define $\Psi = \begin{pmatrix} \psi_L \\ \psi_R \end{pmatrix}$ and $\gamma_\mu = \begin{pmatrix} 0 & \sigma_\mu \\ \bar{\sigma}_\mu & 0 \end{pmatrix}$:

$$(i\gamma_\mu \partial^\mu - m)\Psi = 0 \quad (3.9)$$

This is the Dirac equation (in the Weyl basis of gamma matrices, to be precise). The two fermions now behave as a cohesive, inseparable unit called a Dirac fermion. The four-component vector Ψ is called a Dirac spinor.

However, there is another way to add mass, called Majorana mass:

$$\begin{cases} i\bar{\sigma}_\mu \partial^\mu \psi_L = M_L \chi_R \\ i\sigma_\mu \partial^\mu \psi_R = M_R \chi_L \end{cases} \quad (3.10)$$

Here, $\chi_L \equiv i\sigma_2 \psi_R^*$ and $\chi_R \equiv -i\sigma_2 \psi_L^*$ (where $*$ means complex conjugation). Adding Majorana mass instead of Dirac mass lets the two fermions exist and behave independently. However, this option is only available if the fermions are chargeless: $\chi_{L/R}$ is not only of opposite chirality from $\psi_{R/L}$, but also opposite charge, and it can be shown that equation (3.10) violates charge conservation unless the fermions are chargeless. Fermions that satisfy equation (3.10) are called Majorana fermions, and they are typically represented by the four-component Majorana spinors $\Psi_L = \begin{pmatrix} \psi_L \\ \chi_R \end{pmatrix}$ and $\Psi_R = \begin{pmatrix} \chi_L \\ \psi_R \end{pmatrix}$, since we can find these satisfy the Dirac equation*:

$$(i\gamma_\mu \partial^\mu - M_{L/R})\Psi_{L/R} = 0 \quad (3.11)$$

Since $C\Psi^* \equiv i\gamma_2\Psi^* = \begin{pmatrix} 0 & i\sigma_2 \\ -i\sigma_2 & 0 \end{pmatrix}\Psi^*$ is charge conjugate of a Dirac spinor Ψ in the Weyl basis, it can be found that Majorana fermions are their own antiparticles:

$$C \begin{pmatrix} \psi_L^* \\ \chi_R^* \end{pmatrix} = \begin{pmatrix} \psi_L \\ \chi_R \end{pmatrix}, \quad C \begin{pmatrix} \chi_L^* \\ \psi_R^* \end{pmatrix} = \begin{pmatrix} \chi_L \\ \psi_R \end{pmatrix} \quad (3.12)$$

* χ_L and χ_R satisfy their own versions of equation (3.10), which can be found by multiplying the top equation by $i\sigma_2$ and the bottom by $-i\sigma_2$.

Neutrinos are chargeless, so they could have a Majorana mass. But the type I seesaw mechanism[†] arises when we implement both Dirac and Majorana masses:

$$\begin{cases} i\bar{\sigma}_\mu \partial^\mu \tilde{\nu}_L = m\tilde{\nu}_R \\ i\sigma_\mu \partial^\mu \tilde{\nu}_R = m\tilde{\nu}_L + M\tilde{\chi}_L \end{cases} \quad (3.13)$$

Here, $\tilde{\chi}_L \equiv i\sigma_2 \tilde{\nu}_R^*$ as usual, and $m \ll M$. The idea behind this is that we start with a Weyl fermion $\tilde{\nu}_L$ (an active neutrino) and a Majorana fermion $\tilde{\nu}_R$ with mass M (a sterile neutrino), and then add a weak connection between them in the form of a Dirac mass m . Now, if we multiply the top equation by $i\sigma_\mu \partial^\mu$, multiply the bottom equation by $i\bar{\sigma}_\mu \partial^\mu$ and charge conjugate it, and then rewrite both a bit, we get:

$$\begin{cases} (\square^2 + m^2)\tilde{\nu}_L + mM\tilde{\chi}_L = 0 \\ (\square^2 + m^2 + M^2)\tilde{\chi}_L + mM\tilde{\nu}_L = 0 \end{cases}$$

Or, in matrix form:

$$\left[\square^2 + \begin{pmatrix} m^2 & mM \\ mM & m^2 + M^2 \end{pmatrix} \right] \begin{pmatrix} \tilde{\nu}_L \\ \tilde{\chi}_L \end{pmatrix} = 0 \quad (3.14)$$

Here, $\square^2 \equiv \partial_\mu \partial^\mu$ is the d'Alembertian. Equation (3.14) resembles the Klein-Gordon equation:

$$(\square^2 + m^2)\Psi = 0 \quad (3.15)$$

All components of a Dirac or Majorana spinor should satisfy the Klein-Gordon equation, since $(i\gamma_\mu \partial^\mu + m)(i\gamma_\mu \partial^\mu - m) = -(\square^2 + m^2)$. This means by diagonalizing the mass matrix in equation (3.14) and finding its eigenstates, we can get a strong hint for finding the complete mass eigenstates that solve the Dirac equation. Doing so in the limit $m \ll M$ gives one eigenstate $\tilde{\nu}_1$ with mass $m_1 \approx \frac{m^2}{M}$ and one eigenstate $\tilde{\nu}_2$ with mass $m_2 \approx M$. They are related to $\tilde{\nu}_L$ and $\tilde{\chi}_L$ by:

[†]As the name suggests, there are other possible seesaw mechanisms, but this is the simplest one.

$$\begin{pmatrix} \tilde{\nu}_L \\ \tilde{\chi}_L \end{pmatrix} = \begin{pmatrix} \cos \theta & \sin \theta \\ -\sin \theta & \cos \theta \end{pmatrix} \begin{pmatrix} \tilde{\nu}_1 \\ \tilde{\nu}_2 \end{pmatrix}, \quad (3.16)$$

where $\theta \approx \frac{m}{M}$. Now, it can be shown that the Majorana spinors $\nu_1 \equiv \begin{pmatrix} \tilde{\nu}_1 \\ -i\sigma_2 \tilde{\nu}_1^* \end{pmatrix}$ and $\nu_2 \equiv \begin{pmatrix} \tilde{\nu}_2 \\ -i\sigma_2 \tilde{\nu}_2^* \end{pmatrix}$ satisfy $(i\not{\partial} + m_1)\nu_1 = 0^\ddagger$ and $(i\not{\partial} - m_2)\nu_2 = 0$: these are the mass eigenstates. They are related to $\nu = \begin{pmatrix} \tilde{\nu}_L \\ \tilde{\chi}_R \end{pmatrix}$ and $N = \begin{pmatrix} \tilde{\chi}_L \\ \tilde{\nu}_R \end{pmatrix}$ by:

$$\begin{pmatrix} \nu \\ N \end{pmatrix} = \begin{pmatrix} \cos \theta & \sin \theta \\ -\sin \theta & \cos \theta \end{pmatrix} \begin{pmatrix} \nu_1 \\ \nu_2 \end{pmatrix} \quad (3.17)$$

By slightly mixing the active and sterile neutrino with a small Dirac mass m , the active neutrino has gained a mass far smaller than m : the seesaw mechanism neatly explains why the observed masses of the three active neutrinos are so small. Interestingly, it also implies that both active and sterile neutrinos are Majorana particles.

3.2.2 Sterile neutrinos as dark matter

Equation (3.17) also implies that oscillation can take place between active and sterile neutrinos, which makes it possible for sterile neutrinos to decay. One possible decay is:

$$N \rightarrow \nu_\alpha \gamma \quad (3.18)$$

Here, ν_α can be any of the active neutrinos, and a version of the decay where an antineutrino is produced is also possible, assuming sterile neutrinos are Majorana particles[§]. A lowest-order Feynman diagram of the decay (3.18) can be seen in figure 3.1, but another diagram where the W^+ emits the photon instead of the lepton ℓ^- is also possible. The total decay width of these decays is [30]:

[‡]The fact that there is a plus sign here instead of a minus sign is interesting, but it has no bearing on any physical properties important to our analysis.

[§]Since active neutrinos being Majorana particles is very uncertain, we take active neutrinos and antineutrinos to be different for generality.

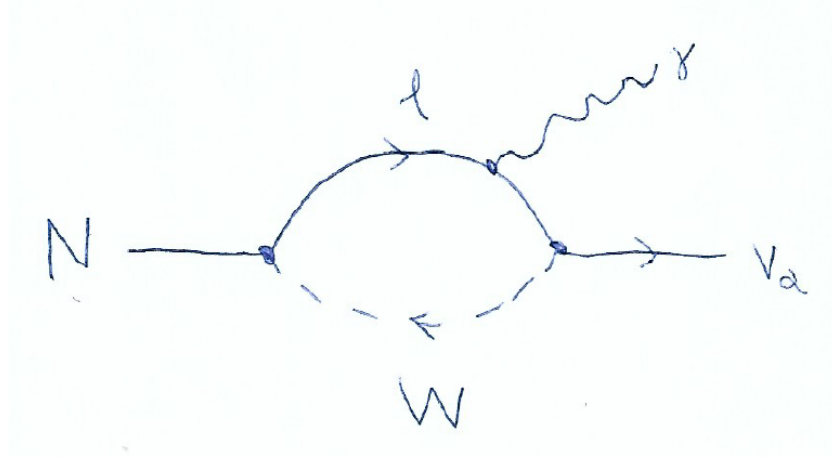


Figure 3.1: Lowest-order Feynman diagram of the decay $N \rightarrow \nu_\alpha \gamma$, where the lepton ℓ emits the photon.

$$\Gamma_{N \rightarrow \nu \gamma} = \frac{9\alpha G_F^2 M^5 \theta^2}{256\pi^4} \approx 5.5 \times 10^{-22} \theta^2 \left(\frac{M}{1 \text{ keV}} \right)^5 \text{ s}^{-1}, \quad (3.19)$$

where G_F is the Fermi coupling constant, α is the fine structure constant and $\theta^2 \equiv \sum_\alpha |\theta_\alpha|^2$, where θ_α is the mixing angle between N and ν_α .

An important property of this decay is that it always produces photons with an energy of $\frac{1}{2}M$ with respect to the inertial frame of the sterile neutrino since it is a two-body decay. This means that dark matter halos should emit faint monochromatic radiation if they contain sterile neutrinos. Such radiation, with an energy of around 3.5 keV, was eventually discovered in 2014 by two independent groups [31–33], and has since been measured in many different systems [34–40]. This suggests dark matter could at least partially consist of sterile neutrinos with a mass of around 7 keV.

For sterile neutrinos with a mass that is less than twice the electron mass, such as the one that is theorized to produce the 3.5 keV radiation, the most probable decay is:

$$N \rightarrow \nu_\alpha \nu_\beta \bar{\nu}_\beta, \quad (3.20)$$

where ν_α and ν_β can be any combination of flavors, and $\bar{\nu}_\alpha$ can also be an antineutrino. A lowest-order Feynman diagram of decay (3.20) can be

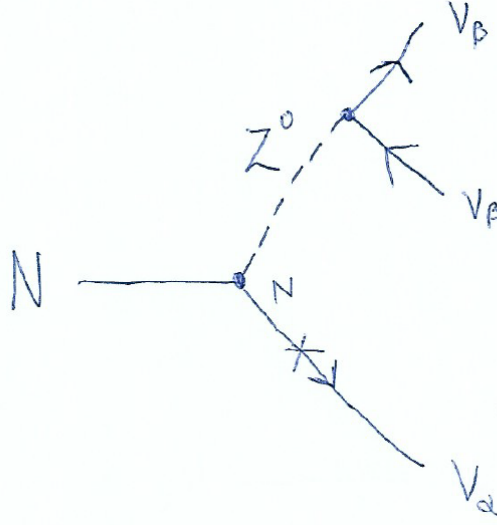


Figure 3.2: Lowest-order Feynman diagram of the decay $N \rightarrow \nu_\alpha \nu_\beta \bar{\nu}_\beta$, where the sterile neutrino emits the Z^0 boson before transforming into ν_α .

seen in figure 3.2, but another diagram where ν_α emits the Z^0 boson also exists. The total decay width of these decays is given by [30]:

$$\Gamma_{N \rightarrow 3\nu} = \frac{G_F^2 M^5 \theta^2}{96\pi^3} \approx 6.7 \times 10^{-20} \theta^2 \left(\frac{M}{1 \text{ keV}} \right)^5 \text{ s}^{-1}, \quad (3.21)$$

about 128 times as likely as decay (3.18).

One condition for a particle to be a dark matter candidate is that their mean lifetime must be around or longer than the age of the universe. The latest data from the Planck satellite tell us this is $t_U = 4.352 \times 10^{17}$ s [41]. Demanding $\Gamma_{N \rightarrow 3\nu} < \frac{1}{t_U}$ now gives us:

$$\theta^2 < 33 \left(\frac{1 \text{ keV}}{M} \right)^5 = 2.0 \times 10^{-3} \quad (3.22)$$

As we will see later, far stricter upper bounds on θ^2 have been calculated for sterile neutrino dark matter, so the stability requirement is certainly satisfied.

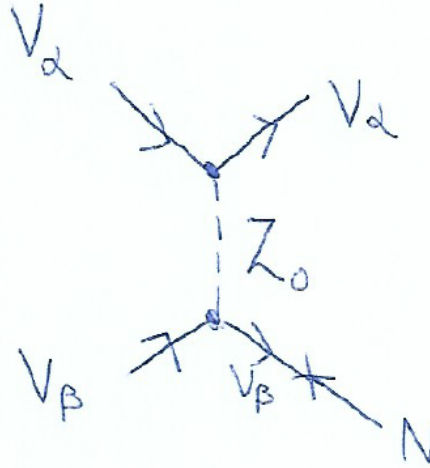


Figure 3.3: Lowest-order Feynman diagram of the process $\nu_\alpha \nu_\beta \rightarrow \nu_\alpha N$, one of the scattering processes that produced sterile neutrinos in the early universe (any of the active neutrinos can also be an antineutrino).

3.2.3 Sterile neutrinos as Warm Dark Matter

Evidently, if sterile neutrinos exist, they have to have been produced at some point in the life of the universe. One way this happened is by scatterings: when two active neutrinos scatter from each other due to the weak interaction, there is a chance one of them "flips over" into a sterile neutrino during the process due to mixing: figure 3.3 shows a Feynman diagram of such a process. The decay width of this process is proportional to (assuming just one active flavor for simplicity of argument) [30]:

$$\Gamma_N \propto G_F^2 T^5 \sin^2(\theta) \quad (3.23)$$

The temperature dependence comes from the fact that scattering is more likely at higher temperatures. From this, one would naively think that sterile neutrino production increases as temperature increases, and that most sterile neutrinos were produced immediately after the Big Bang. However, things are not quite that simple. During the early stages of the universe, it was filled with a thick primordial plasma. This medium strongly affected particle interactions, and, in particular, effectively altered the active-sterile mixing angles, decreasing them for high temperatures: we have to replace the base mixing angle θ with an effective mixing angle θ_m that is still

roughly proportional to θ [30]. Most sterile neutrinos were thus produced at some intermediate temperature, where $T^5 \sin^2(\theta_m)$ peaks. For keV-mass sterile neutrinos, this happened at temperatures around $0.1 - 1$ GeV [30] (θ_m is mass-dependent). Since this is far higher than 7 keV, this means most sterile neutrinos in the universe were born with relativistic momenta. Because Hot Dark Matter has been excluded by measurement [15], this means sterile neutrinos are a Warm Dark Matter candidate: if dark matter consists of sterile neutrinos, those sterile neutrinos must have cooled down to non-relativistic momenta before structure formation.

Whether dark matter is warm or cold can be discovered by studying the structure of the universe today. A quantity important for such an analysis is the free streaming length of a dark matter particle:

$$\lambda_{fs}(t_f) = a(t_f) \int_{t_i}^{t_f} \frac{v(t')}{a(t')} dt', \quad (3.24)$$

the average distance the particle travelled from its production to structure formation, corrected for cosmic expansion (with the scale factor $a(t)$). Since dark matter played a large role in structure formation, few structures of scales below λ_{fs} would have been able to form, since clumps of dark matter on those scales would have been washed out due to dark matter particles free streaming away from each other. λ_{fs} increases with average particle velocity, so WDM particles have a larger free streaming length than CDM particles. For sterile neutrinos with keV-scale mass, the free streaming length has been found to be around 1 Mpc [30], which is around the scale of the average galaxy. This means finding out if dark matter is warm or cold can be done by studying the abundance of structures below this scale in the universe.

Most current constraints on the mass of dark matter sterile neutrinos and their mixing angle are summarized in figure 3.4. Together, these bounds leave little wiggle room for the possible properties of sterile neutrino dark matter. However, these bounds have all been obtained while assuming dark matter entirely consists of sterile neutrinos. In the next chapter, we will investigate how these bounds change if only a fraction of all dark matter consists of sterile neutrinos, and try to broaden the possible parameter space of sterile neutrino dark matter in the process.

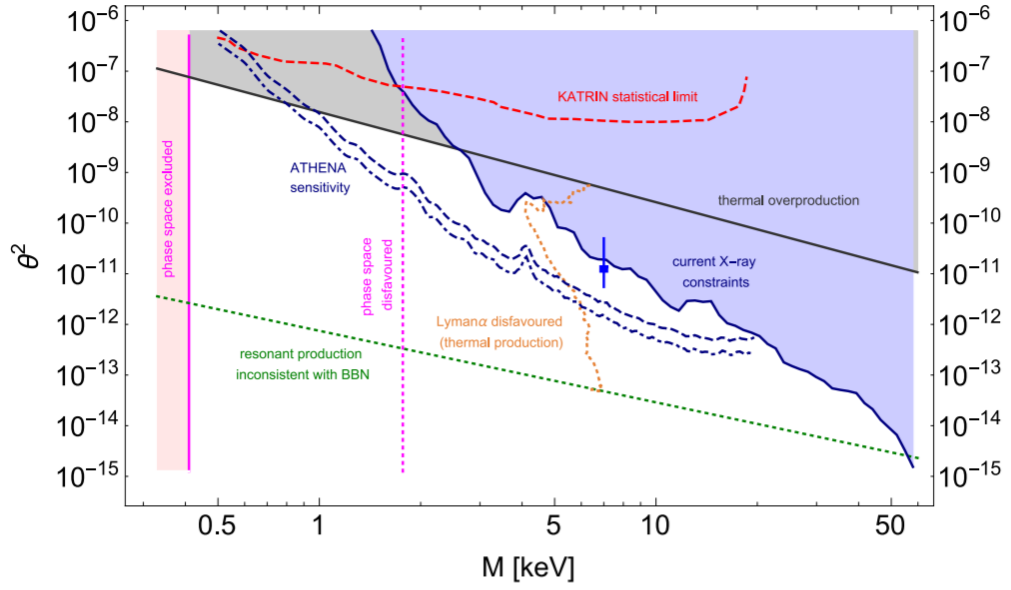


Figure 3.4: Most of the current keV-scale bounds on the $M - \theta^2$ parameter space of dark matter sterile neutrinos assuming dark matter entirely consists of sterile neutrinos. Solid lines indicate mostly model-independent bounds, found using just the basic properties of sterile neutrinos and active-sterile mixing, dotted lines indicate bounds that do not hold for every sterile neutrino model, and dashed and dot-dashed lines indicate estimates of the sensitivity of future experiments. The X-ray constraints, which have been made half as strict to account for possible measurement errors, have changed slightly since the creation of this figure in 2019, but not significantly [42]. The blue data point represents the sterile neutrino properties implied by the 3.5 keV line. A more in-depth explanation of each bound can be found in the original source, Ref. [30].

Sterile neutrinos as a fraction of dark matter

To investigate the change in the available sterile neutrino parameter space if only a fraction of dark matter consists of sterile neutrinos, we will define the sterile neutrino mass fraction:

$$\chi_N \equiv \frac{\rho_N}{\rho_{DM}}, \quad (4.1)$$

where ρ_N and ρ_{DM} are the mass densities of sterile neutrino dark matter and all dark matter, respectively. If we look at a volume in space and measure the total mass of the dark matter in it, we expect that a fraction χ_N of it will be due to sterile neutrinos. We will assume this fraction is the same for all galaxies and clusters, and we will investigate the effect varying this parameter has on the three model-independent bounds in figure 3.4: the Tremaine-Gunn bound (pink), the X-ray constraints (blue), and the thermal overproduction bound (black).

4.1 Tremaine-Gunn bound

The Tremaine-Gunn bound has been previously derived for the $\chi_N = 1$ case in section 2.2, and the derivation is the same for all values of the fraction until equation (2.2):

$$\frac{\hbar}{m_N} \sqrt[3]{\frac{3\pi^2 N_N}{V}} < \sqrt{\frac{2GM}{R}}, \quad (4.2)$$

where N_N is the number of sterile neutrinos in the galaxy. Now, the relation $N_N = \frac{M}{m_N}$ only holds if $\chi_N = 1$: for the general case, we have to take $N_N = \frac{\chi_N M}{m_N}$, which leads to the new Tremaine-Gunn bound:

$$m_N^4 > \frac{9\pi\hbar^3 \chi_N}{8\sqrt{2}G^{3/2}M^{1/2}R^{3/2}} \quad (4.3)$$

As we can see, the bound on m_N is only weakly sensitive to χ_N : it scales with a factor $\chi_N^{1/4}$. In figure 3.4, the pink bound will move to the left if χ_N decreases, becoming less strict.

4.2 X-ray constraints

As discussed in section 3.2.2, sterile neutrinos can decay into an active neutrino and a photon with an energy of $\frac{1}{2}m_N$ in to the inertial frame of the sterile neutrino. This means information about sterile neutrino dark matter can be gained by measuring the radiation coming from dark matter halos, which comes in the form of X-rays for keV-scale sterile neutrino masses. These measurements are done by measuring the flux of the X-rays of each energy coming from a dark matter halo, extracting the radiation from other sources in some way (typically by using reference data from another system or a simulation), and checking if certain X-ray energies have a significantly larger flux than the rest. So far, this has only succeeded for the 3.5 keV line: for the other energies, an upper bound on the active-sterile mixing angle θ as a function of m_N has been calculated by using the error margins of the measurements and the fact that no significant flux spikes were measured.

Now, the flux of decay radiation from a dark matter halo is proportional to the sterile neutrino column number density $n_{N,c}$ (number density integrated over the line of sight) in the halo and the decay width $\Gamma_{N \rightarrow \nu \gamma}$, which is in turn proportional to m_N^5 and θ^2 (see equation (3.19)):

$$F_{\text{decay}} \propto n_{N,c} m_N^5 \theta^2,$$

or:

$$F_{\text{decay}} \propto \rho_{N,c} m_N^4 \theta^2, \quad (4.4)$$

since mass densities and thus column mass densities are the quantities we can actually measure. The X-ray constraints on θ^2 were found by assuming $\chi_N = 1$, and thus $\rho_{N,c} = \rho_{DM,c}$. However, in general, $\rho_{N,c} = \chi_N \rho_{DM,c}$, and all constraints found actually apply to $\chi_N \theta^2$, since we measure $\rho_{DM,c}$ and not $\rho_{N,c}$. So, if θ_X^2 is an upper bound on θ^2 found by X-ray measurements and while assuming $\chi_N = 1$, we have:

$$\theta^2 < \frac{\theta_X^2}{\chi_N} \quad (4.5)$$

As we can see, X-ray bounds on θ^2 scale with a factor χ_N^{-1} , a stronger effect than with than the Tremaine-Gunn bound. In figure 3.4, the blue bound will move upward if α_N decreases, becoming less strict. Since the θ^2 -estimate for the 3.5 keV line was found using similar methods [32], it scales in the same way.

4.3 Thermal overproduction

The thermal overproduction bound was obtained as follows: assuming all sterile neutrinos were produced by scattering as described in section 3.2.3, and assuming $\chi_N = 1$, the black line in figure 3.4 must describe the relationship between m_N and θ^2 of the dark matter sterile neutrino in order to explain the observed dark matter mass density in the universe. However, not all sterile neutrinos were produced by this mechanism, so the black line is a mass-dependent upper bound on θ^2 instead. The bound was obtained by finding a bound:

$$m_N \Gamma_{N,max} < C, \quad (4.6)$$

where $\Gamma_{N,max}$ is the width of the scattering process at the maximum effective mixing angle θ_m (see equation (3.23) and the discussion after it), so that no more mass is produced than observed, and then solving for θ^2 using the fact that $\Gamma_{N,max}$ is approximately proportional to θ^2 . But if only a fraction χ_N of the mass of dark matter consists of sterile neutrinos, the bound C must be multiplied by χ_N . So, if θ_T^2 is a thermal overproduction bound on θ^2 if $\chi_N = 1$, then we have:

$$\theta^2 < \chi_N \theta_T^2 \quad (4.7)$$

This bound actually scales with a factor χ_N , in contrast to the X-ray constraints. In figure 3.4, the black bound will move downward, becoming stricter.

Figure 4.1 illustrates the dependence of the three bounds and the 3.5 keV line data on χ_N . As we can see, a broader keV mass range becomes available as χ_N decreases, but the possible mixing angle range becomes more restricted if χ_N becomes small enough.

The difference in behaviour between the X-ray constraints and the thermal overproduction bound has an interesting consequence. As we can see in figure 4.1, the calculated mixing angle of the 3.5 keV line and the thermal overproduction bound will move closer to each other as χ_N decreases, meeting at a value of about $\theta^2 \approx 10^{-10}$ when approximately $\chi_N \approx 10^{-1}$: if χ_N becomes even smaller, the thermal overproduction bound will exclude the 3.5 keV line. Therefore, if the 3.5 keV line indeed belongs to a sterile neutrino with mass $m_N = 7$ keV, the data in figure 3.4 immediately imply a lower bound on χ_N of approximately:

$$\chi_N \gtrsim 0.1 \quad (4.8)$$

In other words, at least 10% of the mass of dark matter must consist of sterile neutrinos. This is a very rough estimate due to the large error margin on the value of θ^2 corresponding to the 3.5 keV line, so better data is needed to calculate a more exact lower bound.

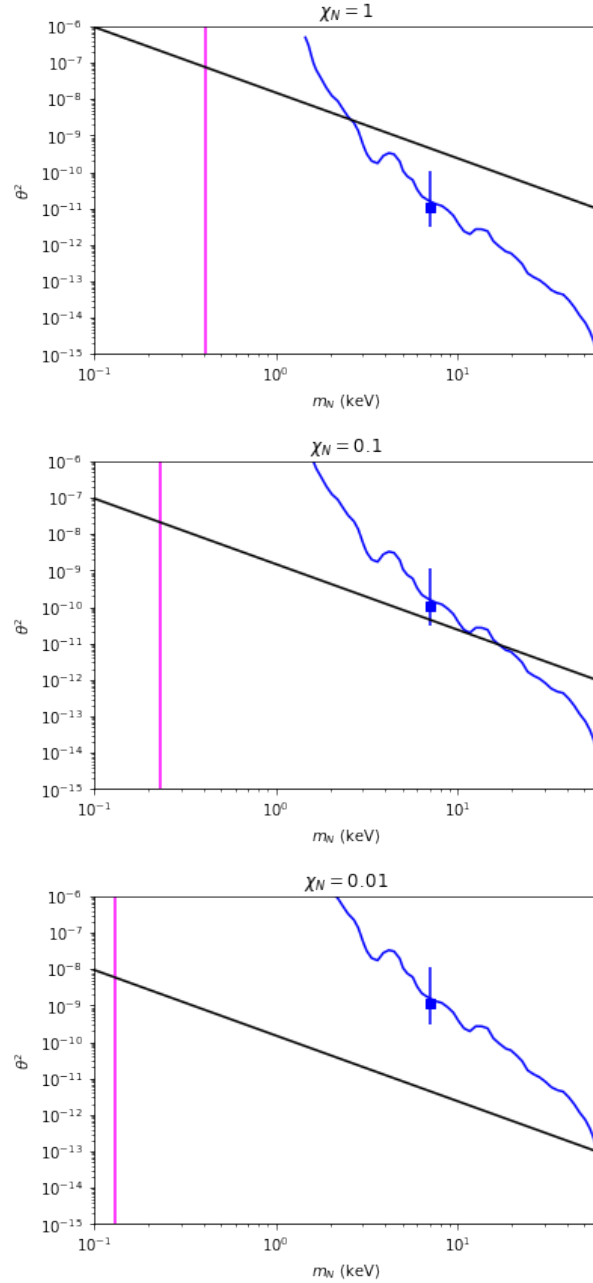


Figure 4.1: Log-log plots roughly illustrating the change in the Tremaine-Gunn bound (magenta line), the X-ray constraints (blue line), the overproduction bound (black line), and the 3.5 keV line data (blue data point) with χ_N , where χ_N is chosen to be 1, 0.1 and 0.01, respectively.

Discussion and conclusion

Sterile neutrinos are a solid candidate for being dark matter. They satisfy all the necessary properties (chargeless, massive, lifetime longer than the age of the universe, production mechanisms and interactions lead to predictions that align with astrophysical and cosmological measurements), and evidence has already been found that could point to their existence (the 3.5 keV line), although it is not yet conclusive.

The greatest weakness of sterile neutrinos is, however, their rather restricted parameter space as a dark matter particle due to various experimental bounds, as can be seen in figure 3.4. In this thesis, we have shown that some more wiggle room for the mass m_N and the active-sterile mixing angle θ of dark matter sterile neutrinos can be gained by considering the possibility that dark matter consists of other particles in addition to sterile neutrinos. The most interesting result of this analysis, however, is that a lower bound on the percentage χ_N of the dark matter mass density that is due to sterile neutrinos can be found if the 3.5 keV line is truly caused by sterile neutrino decay: approximately 10%.

Of course, to get a a more accurate lower bound and more accurate description of the dependence of the sterile neutrino parameter space on the mass percentage, more research must be done. The sensitivity of other bounds to χ_N can be investigated: for example, the more model-dependent bounds in figure 3.4 can be considered. Furthermore, more accurate measurements on the intensity of the 3.5 keV line, and thus the value of θ corresponding to it, can be conducted. This, in addition to improving the accuracy of the overproduction bound by doing more accurate measure-

ments of the dark matter density in the universe, can lead to a sharper lower bound on the mass percentage. This may give us a better understanding of the composition of dark matter, and help find out if the 3.5 keV line is truly the sterile neutrino dark matter signal it is hypothesized to be.

Acknowledgements

I would like to thank my supervisor, Alexey Boyarsky, for giving me the opportunity to do this project and helping me over its course. I would also like to thank Maksym Ovchynnikov, Alexey Mikulenko and Nikyta Shchutskyi for monitoring my progress, for giving me feedback and for always being available to help me through the problems I encountered.

Bibliography

- [1] J. de Swart, G. Bertone, and J. van Dongen, *How Dark Matter Came to Matter*, *Nature Astronomy* **1** (2017).
- [2] F. Zwicky, *Die Rotverschiebung von extragalaktischen Nebeln*. (German) [*The redshift of extragalactic nebulae*], *Helvetica Physica Acta* **6**, 110 (1933).
- [3] S. M. Faber and R. E. Jackson, *Velocity dispersions and mass-to-light ratios for elliptical galaxies*, *The Astrophysical Journal* **204**, 668 (1975).
- [4] E. Corbelli and P. Salucci, *The extended rotation curve and the dark matter halo of M33*, *Monthly Notices of the Royal Astronomical Society* **311**, 441 (2000).
- [5] A. D. Lewis, D. A. Buote, and J. T. Stocke, *Chandra Observations of A2029: The Dark Matter Profile Down to below $0.01r_{vir}$ in an Unusually Relaxed Cluster*, *The Astrophysical Journal* **586**, 135 (2002).
- [6] I. Ferreras, P. Saha, L. L. R. Williams, and S. Burles, *Mapping the Distribution of Luminous and Dark Matter in Strong Lensing Galaxies*, *Proceedings of the International Astronomical Union* **3**, 206 (2007).
- [7] D. Clowe, M. Bradac, A. H. Gonzalez, M. Markevitch, S. W. Randall, C. Jones, and D. Zaritsky, *A direct empirical proof of the existence of dark matter*, *The Astrophysical Journal Letters* **648**, L109 (2006).
- [8] M. Milgrom, *A modification of the Newtonian dynamics as a possible alternative to the hidden mass hypothesis*, *The Astrophysical Journal* **270**, 365 (1983).

-
- [9] M. Milgrom, *A modification of the Newtonian dynamics - Implications for galaxies*, *The Astrophysical Journal* **270**, 371 (1983).
- [10] M. Milgrom, *A modification of the Newtonian dynamics - Implications for galaxy systems*, *The Astrophysical Journal* **270**, 384 (1983).
- [11] P. H. Frampton, M. Kawasaki, F. Takahashi, and T. T. Yanagida, *Primordial Black Holes as All Dark Matter*, *Journal of Cosmology and Astroparticle Physics* **2010** (2010).
- [12] S. Clesse and J. García-Bellido, *Seven hints for primordial black hole dark matter*, *Physics of the Dark Universe* **22**, 137 (2018).
- [13] B. C. Lacki and J. F. Beacom, *Primordial Black Holes as Dark Matter: Almost All or Almost Nothing*, *The Astrophysical Journal Letters* **720**, L67 (2010).
- [14] P. A. R. Ade et al., *Planck 2013 results. I. Overview of products and scientific results*, *Astronomy & Astrophysics* **571** (2014).
- [15] A. Sokolenko, *Enlightening the Dark*, PhD thesis, University of Oslo, 2019.
- [16] M. G. Aartsen et al., *Searches for Sterile Neutrinos with the IceCube Detector*, *Physical Review Letters* **117** (2016).
- [17] A. A. Aguilar-Arevalo et al., *Significant Excess of Electronlike Events in the MiniBooNE Short-Baseline Neutrino Experiment*, *Physical Review Letters* **121** (2018).
- [18] A. Stebbins and G. Krnjaic, *New Limits on Charged Dark Matter from Large-Scale Coherent Magnetic Fields*, *Journal of Cosmology and Astroparticle Physics* **2019** (2019).
- [19] S. Tremaine and J. E. Gunn, *Dynamical Role of Light Neutral Leptons in Cosmology*, *Physical Review Letters* **42**, 407 (1979).
- [20] A. Boyarsky, O. Ruchayskiy, and D. Iakubovskyi, *A lower bound on the mass of dark matter particles*, *Journal of Cosmology and Astroparticle Physics* **2009** (2009).
- [21] P. J. McMillan, *The mass distribution and gravitational potential of the Milky Way*, *Monthly Notices of the Royal Astronomical Society* **465**, 76 (2016).

-
- [22] A. J. Deason, A. Fattahi, C. S. Frenk, R. J. J. Grand, K. A. Oman, S. Garrison-Kimmel, C. M. Simpson, and J. F. Navarro, *The Edge of the Galaxy*, Monthly Notices of the Royal Astronomical Society (2020), accepted manuscript.
- [23] N. Palanque-Delabrouille, C. Yèche, J. Baur, C. Magneville, G. Rossi, J. Lesgourgues, A. Borde, E. Burtin, J.-M. LeGoff, J. Rich, M. Viel, and D. Weinberg, *Neutrino masses and cosmology with Lyman-alpha forest power spectrum*, Journal of Cosmology and Astroparticle Physics **2015** (2015).
- [24] B. Pontecorvo, *Mesonium and Antimesonium*, Journal of Experimental and Theoretical Physics **6**, 429 (1957).
- [25] Z. Maki, M. Nakagawa, and S. Sakata, *Remarks on the Unified Model of Elementary Particles*, Progress of Theoretical Physics **28**, 870 (1962).
- [26] B. Pontecorvo, *Neutrino Experiments and the Problem of Conservation of Leptonic Charge*, Journal of Experimental and Theoretical Physics **26**, 984 (1968).
- [27] Y. Fukuda et al., *Evidence for Oscillation of Atmospheric Neutrinos*, Physical Review Letters **81**, 1562 (1998).
- [28] C. Giganti, S. Lavignac, and M. Zito, *Neutrino oscillations: The rise of the PMNS paradigm*, Progress in Particle and Nuclear Physics **98**, 1 (2018).
- [29] M. Tanabashi et al., *Review of Particle Physics*, Physical Review D **98** (2018), Chapter 14.
- [30] A. Boyarsky, M. Drewes, T. Lasserre, S. Mertens, and O. Ruchayskiy, *Sterile neutrino Dark Matter*, Progress in Particle and Nuclear Physics **104**, 1 (2019).
- [31] E. Bulbul, M. Markevitch, A. Foster, R. K. Smith, M. Loewenstein, and S. W. Randall, *Detection of An Unidentified Emission Line in the Stacked X-ray spectrum of Galaxy Clusters*, The Astrophysical Journal **789**, 1 (2014).
- [32] A. Boyarsky, O. Ruchayskiy, D. Iakubovskiy, and J. Franse, *Unidentified Line in X-Ray Spectra of the Andromeda Galaxy and Perseus Galaxy Cluster*, Physical Review Letters **113** (2014).
-

- [33] A. Boyarsky, J. Franse, D. Iakubovskiy, and O. Ruchayskiy, *Checking the Dark Matter Origin of a 3.53 keV Line with the Milky Way Center*, *Physical Review Letters* **115** (2015).
- [34] O. Ruchayskiy, A. Boyarsky, D. Iakubovskiy, E. Bulbul, D. Eckert, J. Franse, D. Malyshev, M. Markevitch, and A. Neronov, *Searching for decaying dark matter in deep XMMNewton observation of the Draco dwarf spheroidal*, *Monthly Notices of the Royal Astronomical Society* **460**, 1390 (2016).
- [35] J. Franse, E. Bulbul, A. Foster, A. Boyarsky, M. Markevitch, M. Bautz, D. Iakubovskiy, M. Loewenstein, M. McDonald, E. Miller, S. W. Randall, O. Ruchayskiy, , and R. K. Smith, *Radial Profile of the 3.55 keV line out to R_{200} in the Perseus Cluster*, *The Astrophysical Journal* **829**, 1 (2016).
- [36] O. Urban, N. Werner, S. W. Allen, A. Simionescu, J. S. Kaastra, and L. E. Strigari, *A Suzaku Search for Dark Matter Emission Lines in the X-ray Brightest Galaxy Clusters*, *Monthly Notices of the Royal Astronomical Society* **451**, 2447 (2015).
- [37] A. Neronov, D. Malyshev, and D. Eckert, *Decaying dark matter search with NuSTAR deep sky observations*, *Physical Review D* **94** (2016).
- [38] K. Perez, K. C. Y. Ng, J. F. Beacom, C. Hersh, S. Horiuchi, and R. Krivonos, *Almost closing the ν MSM sterile neutrino dark matter window with NuSTAR*, *Physical Review D* **95** (2017).
- [39] D. Iakubovskiy, E. Bulbul, A. R. Foster, D. Savchenko, and V. Sadova, *Testing the origin of 3.55 keV line in individual galaxy clusters observed with XMM-Newton*, pre-published on arXiv.org, 2015.
- [40] N. Cappelluti, E. Bulbul, A. Foster, P. Natarajan, M. C. Urry, M. W. Bautz, F. Civano, E. Miller, and R. K. Smith, *Searching for the 3.5 keV Line in the Deep Fields with Chandra: The 10 Ms Observations*, *The Astrophysical Journal* **854**, 1 (2018).
- [41] N. Aghanim et al., *Planck 2018 results. VI. Cosmological parameters*, forthcoming article in *Astronomy & Astrophysics*, 2018.
- [42] B. M. Roach, K. C. Y. Ng, K. Perez, J. F. Beacom, S. Horiuchi, R. Krivonos, and D. R. Wik, *NuSTAR Tests of Sterile-Neutrino Dark Matter: New Galactic Bulge Observations and Combined Impact*, *Physical Review D* **101** (2020).